J Mater Sci (2011) 46:634–640
DOI 10.1007/s10853-010-4785-9

Gelatin-assisted porous expansion of mesoporous silica

Lu Wang · Xiaoheng Liu · Xin Wang · Xujie Yang · Lude Lu

Received: 26 March 2010 / Accepted: 21 July 2010 / Published online: 4 August 2010
© Springer Science+Business Media, LLC 2010

Abstract In this study, we report the pore expansion effect of gelatin, a common amphoteric biological protein, on the hexagonal mesoporous silica materials. Tetraethyl orthosilicate (TEOS) was used as silica source and the nonionic surfactant P123 ($EO_{20}PO_{70}EO_{20}$) as template. The microstructure characters of products were investigated by low-angle X-ray diffraction (LAXRD), transmission electron microscope (TEM), and N_2 adsorption–desorption measurements. The results show that the products prepared with gelatin have the mild expansion ratios of 29–39% and 5–22% in pore diameter and pore volume, respectively. The specific surface area of products ranges from 445 to 590 $m^2\ g^{-1}$. Moreover, it is revealed that the presence of gelatin did not change the intact 2D-hexagonal mesoporous structure of materials. The ultraviolet–visible absorption spectroscopy (UV–Vis) analysis indicates that there is an interaction between the oxygen atoms of P123 and gelatin molecules. The pore expansion may be because the gelatin can interact with the hydrophilic sides of P123 micelles via hydrogen bonds interaction, which is different from the reported pore expansion mechanisms for other systems.

Introduction

Ordered mesoporous silica materials have widespread potential applications in fields such as chemical catalysis [1], drug delivery, [2] and selective separation [3] due to their controllable pore sizes and regular structures. Generally surfactants, either ionic or nonionic ones, are of great help in directing the pores formation during the synthesis of these materials. One typical example is the application of nonionic amphiphilic triblock copolymers surfactant P123 ($EO_{20}PO_{70}EO_{20}$) as template to the preparation of SBA-15 [4–8], which is characterized by its strong structural regularity, thick pore walls, and notable hydrothermal stability [9]. It should be noted that one big problem for the mesoporous materials is the difficulty in manipulation of the pore sizes. Nevertheless the pore sizes are of great essential in selective separation of biological macromolecules, proteins, or ions and so on [3, 10]. Up to now, the main reported strategies to control the pore sizes can be carried out by either using the swelling agents or double surfactant approach [11]. The pore expansion mechanisms for the former are mainly based on the fact that the hydrophobic chains of surfactants can interact with the whole swelling agent molecules such as benzene, 1,3,5-trimethylbenzene [12], and decane [13]. The latter enhances the pore size through the self-organization into concentric cylinders inside the pore channels of the double surfactant due to the favorable hydrophobic interactions between their hydrocarbon chains. Besides, Sörensen et al. [14] have studied the porous expansion of polypropylene glycol in F127 ($EO_{106}PO_{70}EO_{106}$) templates system. However, no study on the application of amphoteric macromolecular protein on expanding porous structure has been reported at present.

In the past, lots of studies on the properties and utilizations of gelatin, a denatured polypeptide obtained from acid-treated or alkali-treated collagen [15], have been undertaken in alimentary, pharmaceutic, and biological researches [16–21]. Gelatin has a heterogeneous distribution of at least 18 amino acids, which contains mainly glycine (about 27%), praline and hydroxyproline (about

L. Wang · X. Liu · X. Wang (✉) · X. Yang · L. Lu
Key Laboratory for Soft Chemistry and Functional Materials, Nanjing University of Science and Technology, Ministry of Education, Nanjing 210094, China
e-mail: njustw@gmail.com

25%), glutamic acid (about 10%), arginine (about 8%), alanine (about 9%), aspartic acid (about 6%), and other amino acids (about 10%) [22–24]. When the temperature is above 37 °C, gelatin usually is considered to be a linear random-coil polymer in aqueous solution [24–27]. It is well known that gelatin–surfactants interactions are wide existing, no matter the latter being ionic or nonionic ones [28]. Gelatin was often used with various surfactants to improve stability, lower surface tension, and modify rheological properties of the final products [29]. For instance, the electrostatic adsorption of gelatin-anionic surfactant has been successfully utilized to prepare the zirconia nanodisks [30].

Herein, we made an attempt to use gelatin as swelling agent for adjusting the pore size of mesoporous materials. In this article, 2D-hexagonal ordered mesoporous silica materials were prepared with P123 ($EO_{20}PO_{70}EO_{20}$) template in a reproducible non-hydrothermal method. It is found that gelatin expands the pore diameters and pore volumes of materials in a milder scope, meanwhile the mesoporous structure also remains intact. Furthermore, the pore expansion mechanism of gelatin was also discussed in this article.

Experimental

Materials

Type A gelatin is derived from porcine skin through acid treatment, whose pH value and isoelectric point (IEP) in water are around 5 and 8, respectively [31]. According to a previous report [32], there are five ingredients in the gelatin: α_p, α, β, γ, and γ_p chains. The average molecular weight of gelatin is 0.9×10^5. Its average carbon, nitrogen, and hydrogen contents are 40.91, 14.57, and 6.91 wt%, respectively (Elementar Vario MICRO, Germany). Pluronic P123 (Mav 5800) was purchased from Aldrich. The other chemicals were obtained from Shanghai Chemical Reagents. All the chemicals were analytical grade and were used without further purification.

Synthesis

In our synthesis, 1.0 g (0.172 mmol) of P123 and different amounts of gelatin (0.1, 0.2, 0.3, 0.5, 0.7, and 1.0 g) were dissolved in 22.5 g of deionized water and stirred for 30 min. A quantity of 15 g (4 M) of hydrochloric acid (HCl) was added to the solution and stirred for 1 h. Then, 2.225 g (10.680 mmol) of tetraethyl orthosilicate (TEOS) was added and stirred for another 24 h. The whole synthesis was carried out at 38 °C. The molar ratio in the mixture was P123:TEOS:carbon of gelatin:HCl:H_2O = 1:62:20–200:290:7267. The mixture was filtered, washed with deionized water, dried at room temperature, and calcined at 600 °C for 6 h with the heating rate of 1 °C min^{-1}. The products prepared with different molar ratios of carbon in gelatin to P123, 0, 20, 40, 60, 100, 140, and 200, were labeled as neat-P123, 20-$M_{Gelatin:P123}$, 40-$M_{Gelatin:P123}$, 60-$M_{Gelatin:P123}$, 100-$M_{Gelatin:P123}$, 140-$M_{Gelatin:P123}$, and 200-$M_{Gelatin:P123}$, respectively. For the sake of completeness, the product prepared with neat gelatin (1.0 g) was also obtained, labeled as neat-Gelatin.

Characterization

Thermogravimetric measurements were performed on a thermal analyzer of SDT Q600 V8.0 Build 95. Low-angle X-ray diffraction (LAXRD) patterns were obtained on a Rigaku D/MAX-2500 PC using Cu Kα radiation. Transmission electron microscope (TEM) pictures were collected on a JEM-2100 (JEOL) electron microscope. N_2 adsorption–desorption isotherms at 77 K were obtained on a Micromeritics ASAP 2010 apparatus. The samples were degassed at 250 °C overnight before measure. Pore size distributions and pore volumes were determined by the Barret–Joyner–Halenda (BJH) method. Ultraviolet–visible absorption spectroscopy (UV–Vis) was performed on a UV–Vis 1201 spectrophotometer (Beijing Ruili Analytical Instrument Corp, China).

Results

Thermal analysis

The TG–DTA curves of the as-prepared 200-$M_{Gelatin:P123}$ are shown in Fig. 1. In the TG plot, an evident mass loss was recorded in the temperature range of 200–450 °C due to the decomposition of organic species. No pronounced loss of weight can be observed with the elevated temperature. Correspondingly, the DTA curve shows a remarkable exothermic peak at 214 °C. A flat after around 550 °C in the TG plot indicates the complete thermal decomposition. Therefore, 600 °C was selected as the calcination temperature to ensure the complete removal of organic species.

LAXRD patterns and TEM micrographs

Figure 2 shows the LAXRD patterns of neat-P123, neat-Gelatin, and a series products prepared with P123 and gelatin. Previous research confirmed that gelatin can be used as template to prepare the mesoporous silica materials via the multiple hydrogen bonds' interaction between the amide groups on gelatin and the silanol groups on silicate

species [33]. No diffraction peak in the LAXRD pattern of neat-Gelatin demonstrates a possible disordered porous structure, which is identical with the reported result [33]. Except for neat-Gelatin, each pattern exhibits an intense (100) diffraction peaks and two weak (110) and (200) ones, which is characteristic for a 2D-hexagonal phase [34]. Compared to the neat-P123, it is obvious that the 2θ angles of (100) diffraction of other products moved toward the smaller values, indicating the increased pore–pore correlation distance [35]. The corresponding d_{100} values of these products calculated by Bragg Equation $d = \lambda/2Sin\theta$ [36] are listed in Table 1. However, the peak intensity does not decrease when the gelatin amount increases, suggesting that the materials still possess a high structural ordering.

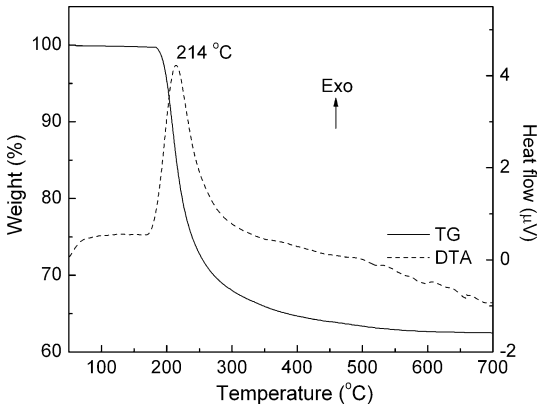

Fig. 1 TG–DTA curves of as-prepared 200-$M_{Gelatin:P123}$

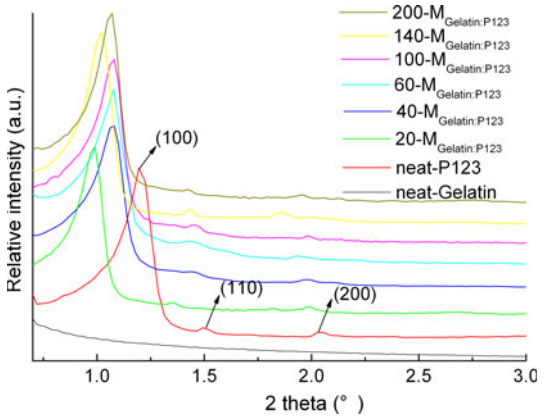

Fig. 2 LAXRD patterns of products

As a representative, Fig. 3a and b provides the TEM images of 20-$M_{Gelatin:P123}$, which exhibit a distinct ordered hexagonal arrangement of pore entrance and an uniform array of pore channel. Its pore diameter and wall thickness are around 4–5 nm and 5–6 nm, respectively. On the other hand, as predicted from LAXRD result, the disordered wormlike mesostructure of neat-Gelatin can be observed clearly in Fig. 3c and d. The disorder pore structure may originate from the irregular and random structure of gelatin.

N_2 adsorption–desorption studies

The N_2 adsorption–desorption isotherms results can offer more detailed information about microstructure properties and are shown in Fig. 4a. Each product displays the type IV adsorption–desorption isotherms for mesoporous structure according to the IUPAC classification [37]. The type H1 hysteresis loop in the isotherms indicates the cylindrical or rodlike geometry of the pores. The relative pressure value at capillary condensation step in the adsorption isotherm for all the products increases in the sequence neat-P123 $<$ 40-$M_{Gelatin:P123}$ $\approx$ 60-$M_{Gelatin:P123}$ $<$ 100-$M_{Gelatin:P123}$ $<$ 140-$M_{Gelatin:P123}$ $<$ 20-$M_{Gelatin:P123}$. Therefore the pore size increases also in the same order. Figure 4b presents the corresponding pore diameter distributions of products. The pore size of each product intensively distributes in a narrow scope of around 3–5 nm. One significant feature for the products prepared with gelatin is their enlarged pore sizes in relative to neat-P123. Furthermore, the increase of pore size follows the identical sequence as observed in N_2 adsorption–desorption isotherms.

Table 1 Sample structural properties

Sample	d_{100} (nm)	a^a (nm)	S^b_{BET} ($m^2\ g^{-1}$)	V^c_P ($cm^3\ g^{-1}$)	P^d (nm)	b^e (nm)	L^f_r
neat-P123	7.8	9.0	504	0.41	3.1	5.9	1
20-$M_{Gelatin:P123}$	8.9	10.3	590	0.48	4.3	6.0	0.62
40-$M_{Gelatin:P123}$	8.2	9.5	472	0.50	4.0	5.5	0.73
60-$M_{Gelatin:P123}$	8.3	9.6	533	0.43	4.0	5.6	0.63
100-$M_{Gelatin:P123}$	8.2	9.5	566	0.44	4.1	5.4	0.61
140-$M_{Gelatin:P123}$	8.7	10.0	445	0.43	4.2	5.8	0.57
200-$M_{Gelatin:P123}$	8.2	9.5	514	0.41	4.1	5.4	0.57

[a] a is the lattice parameter, $a = 2d_{100}/\sqrt{3}$; [b] S_{BET} is the Brunauer–Emmett–Teller (BET) surface area; [c] V_p is the BJH desorption average pore volume; [d] P is the average pore diameter; [e] b is the wall thickness, $b = a - P$; [f] L_r is the relative pore length, $L_r = V_pP_0^2/V_0P^2$, V_0 and P_0 are the average pore volume and average pore diameter of sample neat-P123, respectively

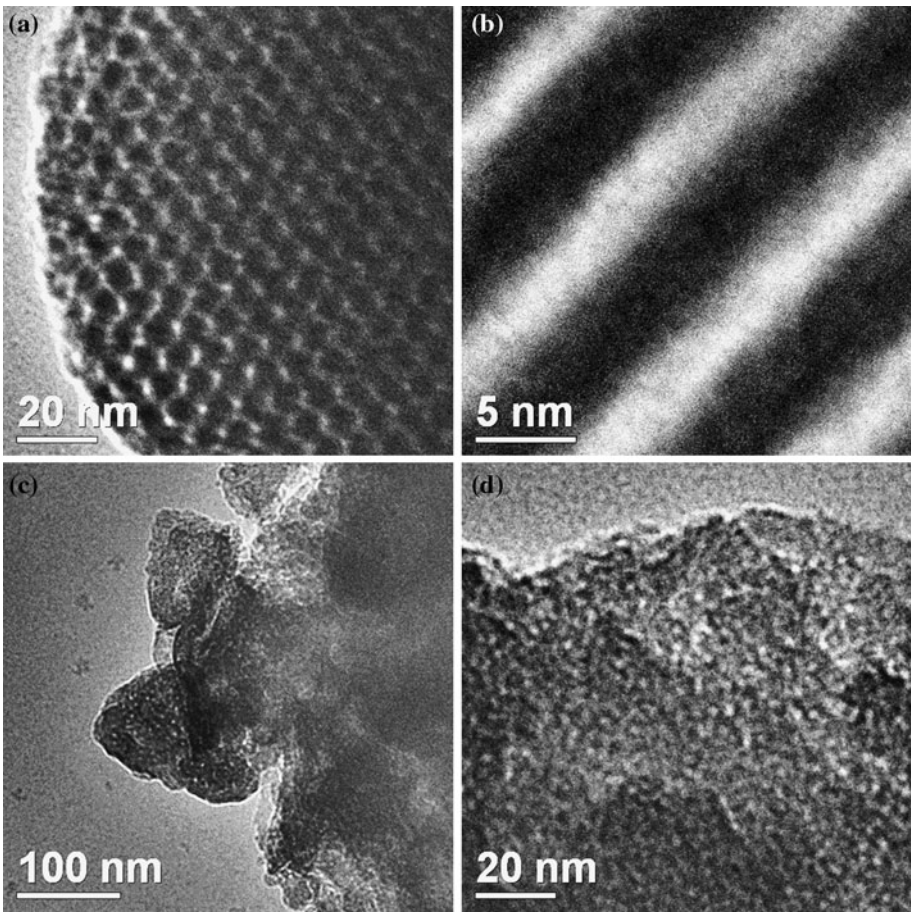

Fig. 3 TEM micrographs of **a** 20-$M_{Gelatin:P123}$ (*front view*), **b** 20-$M_{Gelatin:P123}$ (*side view*), and **c** neat-Gelatin (*large scope view*), **d** neat-Gelatin (*small scope view*)

Table 1 summarizes the textural characters of products, which derived from the above LAXRD and N_2 adsorption–desorption measurements. All the products prepared with gelatin except one give mesoporous materials with the increased pore diameters and pore volumes. In the presence of gelatin, the increase rates of pore diameter and pore volume are 29–39% and 5–22%, respectively. The S_{BET} of products, which has no proportionate relation with the pore size [38–40], distributes in the range of 445–590 $m^2\ g^{-1}$. However, the pore size dose not improve markedly with the growth of the amount of gelatin. This reason can be found in the following mechanism discussion. Besides, the pore sizes and wall thickness of product 20-$M_{Gelatin:P123}$ agree well with the above observations of TEM images.

It can be observed that, with an incremental of the amount of gelatin, the average pore volume ascend initially (20-$M_{Gelatin:P123}$ (0.48 $cm^3 \cdot g^{-1}$) and 40-$M_{Gelatin:P123}$ (0.50 $cm^3 \cdot g^{-1}$)), and then descend. Meanwhile, the average pore length (Table 1) also shows the similar variation tendency on the whole. The molecular association of P123 led to the formation of rodlike P123 micelles. The introduction of excess gelatin into the preparation system reduced the average association degree of P123 molecular to a certain extent, which shortened the average length of rodlike micelles. Take 200-$M_{Gelatin:P123}$ for instance, its average pore volume declines to 0.41 $cm^3\ g^{-1}$, which is equal to that of neat-P123.

UV–Vis absorption spectra

The reaction solutions without silica source for preparing samples were evaluated by UV–Vis absorption spectroscopy. The obtained UV–Vis spectra are represented in Fig. 5a. Curve a shows two characteristic absorption bands of gelatin. The absorption bands of around 242 nm can be ascribed to the $n \rightarrow \pi^*$ electron transition of carbonyl groups on peptide chains. Meanwhile, another band of around 274 nm reflects the $\pi \rightarrow \pi^*$ electron transition of the residues of tryptophan and tyrosine. In curve b, the bands of around 203 nm are associated with the $n \rightarrow \sigma*$ electron transition of lone pair electrons of oxygen of P123. All the other UV–Vis absorption spectra (curves c, d, and e) show the similar absorption patterns. Interestingly, no movement of the absorption at 274 nm and a red shift from 232 nm to 242 nm can be observed when the gelatin amount increases from 0.1 to 1.0 g.

As a representative, Fig. 5b shows the result of peak fitting of curve c in Fig. 5a. A good coincidence can be

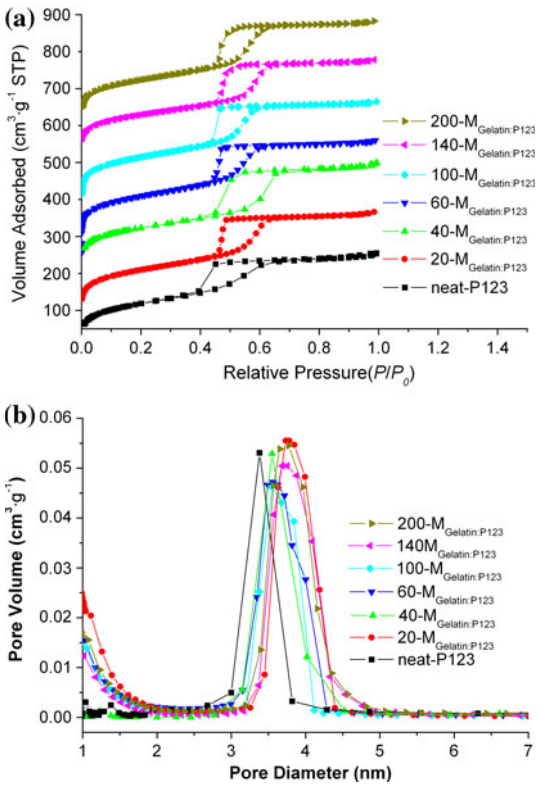

Fig. 4 **a** N_2 adsorption–desorption isotherms at 77 K and **b** the BJH pore size distributions of products determined on the basis of the desorption branches

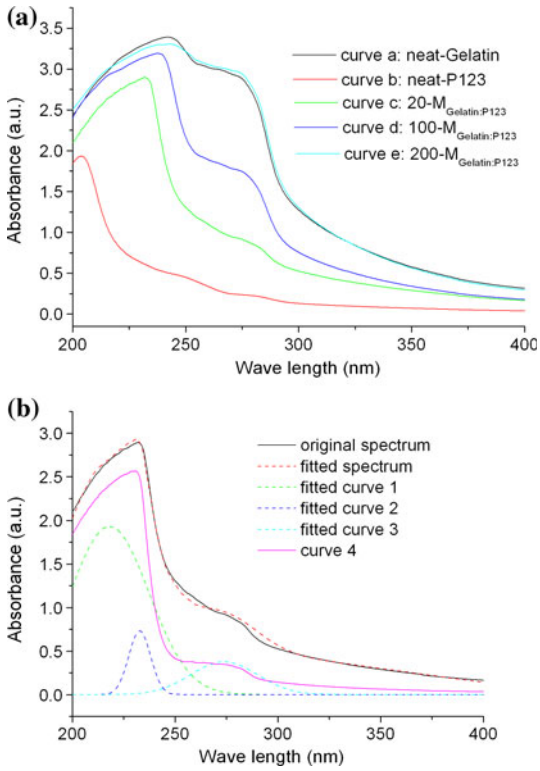

Fig. 5 **a** UV–Vis spectra of the reaction solutions for preparing samples, which contains a certain amount of gelatin and P123 dissolved in 22.5 g of water and 15 g (4 M) of HCl solution. *curve a*: 1.0 g of gelatin and 0 g of P123; *curve b*: 0 g of gelatin and 1.0 g of P123; *curve c*: 0.1 g of gelatin and 1.0 g of P123; *curve d*: 0.5 g of gelatin and 1.0 g of P123; *curve e*: 1.0 g of gelatin and 1.0 g of P123. **b** Peak fitting of *curve c* in Fig. 5a and the UV–Vis absorption spectroscopy of the gelatin solution, which contains 0.1 g of gelatin, 22.5 g of water, and 15 g (4 M) of HCl solution (*curve 4*)

seen between the original spectrum and the fitted one. The original spectrum was decomposed into three Gaussian-type curves 1, 2, and 3. For comparison, the UV–Vis absorption spectroscopy of the 0.1 g of gelatin dissolved in water and HCl solution was also measured (curve 4). The absorption bands of 232 nm in curve 2 and 274 nm in curve 3 are consistent with the positions of absorption bands of gelatin (curve 4). Compared to the characteristic absorption band of P123 (203 nm, curve b in Fig. 5a), a red shift of about 15 nm can be detected for the absorption band around 218 nm in curve 1, which suggests that the electronic states of oxygen atoms in P123 have been varied after gelatin was added into the preparation process.

Discussion

In this study, results of LAXRD and N_2 adsorption–desorption revealed that the addition of macromolecule gelatin can improve the pore size of mesoporous materials, and the UV–Vis results confirm the existence of interaction between oxygen atoms on P123 micelles and gelatin. According to the formation mechanism of mesoporous materials [41, 42], it is presumed that the pore expansion effect may be caused by the changes of P123 micelles after gelatin was introduced.

Gelatin usually possesses a plenty of –COOH and –NH_2 groups on the chain ends, and many –CONH– groups on the peptide chains. In this study, the pH value (0.15) of the reaction system was far below the gelatin IEP (around 8), and gelatin carried positive charges in the whole reaction. On the other hand, when P123 was dissolved in water, the oxygen atoms on ether bonds interacted with the hydrogen atoms of water to form hydrogen bonds. The hydrophilic oxygen atoms and hydrophobic –CH_2CH_2– groups were on external and inner sides of the twisted molecular chains, respectively. Hence, one side of the P123 micelle form by the connected molecular chains was hydrophilic and the other was hydrophobic. As described in Fig. 6, gelatin molecules have the high affinity to interact with the P123 micelles via the hydrogen bonds interactions in two ways: one way is to directly connect the oxygen atoms on the hydrophilic sides of micelles; and the other is to connect the hydrogen atoms of water which linked with the hydrophilic sides of micelles. The entry of gelatin into the hydrophilic sides of micelles increases the overall micelle size. This is completely different from the previous reported expansion

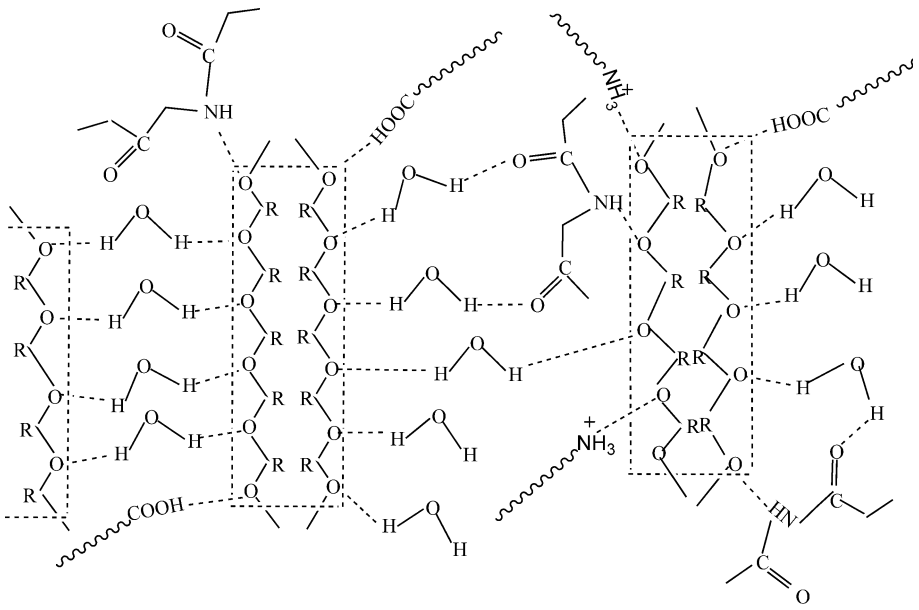

Fig. 6 The schematic diagram of interaction between P123 micelles and gelatin. the parts enclosed by the dotted lines represent P123 chains. R represents alkyl groups

mechanism of hydrophobic chains interaction for hydrocarbon-cationic surfactants or polypropylene glycol-F127 systems, as mentioned in introduction part [12–14]. Because the pore size depends on the size of hydrophobic groups more heavily than that of hydrophilic groups of surfactant micelles [34], the expansion effect of this system is not very obvious although the amount of gelatin increases.

Conclusion

In summary, this study confirms the pore expansion effect of gelatin on the hexagonal mesoporous silica materials. Our primary experimental results suggest the expansion mechanism can be attributed to the gelatin insertion into the hydrophilic sides of micelles through the hydrogen bond interaction. Moreover, the LAXRD, TEM, and N_2 adsorption–desorption analyses proved that there is no loss of pore ordering in the expanded mesoporous materials. This study provided a new exploiting direction for macromolecular protein application in the material fabrication.

Acknowledgments This study was supported by the National Natural Science Foundation of China (No. 50772048) and Natural Science Foundation of China Academy of Engineering Physics (No. 10776014).

References

1. Corma A (1997) Chem Rev 97:2373
2. de Sousa A, Maria DA, de Sousa RG, de Sousa EMB (2010) J Mater Sci 45:1478–1486
3. Yiu HHP, Botting CH, Botting NP, Wright PA (2001) Phys Chem Chem Phys 3:2983
4. Zhao DY, Feng JL, Huo QS, Melosh N, Fredrickson GH, Chmelka BF, Stucky GD (1998) Science 279:548
5. Zhao DY, Sun JY, Li QZ, Stucky GD (2000) Chem Mater 12: 275
6. Borodko Y, Ager JW, Marti GE, Song H, Niesz K, Somorjai GA (2005) J Phys Chem B 109:17386
7. Ruthstein S, Schmidt J, Kesselman E, Talmon Y, Goldfarb D (2006) J Am Chem Soc 128:3366
8. Chao MC, Chang CH, Lin HP, Tang CY, Lin CY (2009) J Mater Sci 44:6453
9. Li FX, Yu F, Li YL, Li RF, Xie KC (2007) Microporous Mesoporous Mater 101:250
10. Algarra M, Jiménez MV, Rodríguez-Castellón E, Jiménez-López A, Jiménez-Jiménez J (2005) Chemosphere 59:779
11. Sayari A, Shee D, Al-Yassir N, Yang Y (2010) Top Catal 53:154–167
12. Luechinger M, Pirngruber GD, Lindlar B, Laggner P, Prins R (2005) Microporous Mesoporous Mater 79:41
13. Zhang FQ, Meng Y, Gu D, Yan Y, Chen ZX, Tu B, Zhao DY (2006) Chem Mater 18:5279
14. Sörensen MH, Corkery RW, Pedersen JS, Rosenholm J, Alberius PC (2008) Microporous Mesoporous Mater 113:1
15. Russell JD, Dolphin JM, Koppang MD (2007) Anal Chem 79:6615
16. Badii F, Howell NK (2009) Food Hydrocoll 23:563
17. Liu HF, Fan HB, Cui YL, Chen YP, Yao KD, Goh JCH (2007) Biomacromolecules 8:1446
18. H Fan, Zhang C, Li J, Bi L, Qin L, Wu H, Hu YY (2008) Biomacromolecules 9:927
19. Lai JY, Lin PK, Hsiue GH, Cheng HY, Huang SJ, Li YT (2009) Biomacromolecules 10:310
20. Sakai S, Yamaguchi S, Takei T, Kawakami K (2008) Biomacromolecules 9:2036
21. Barbetta A, Massimi M, Rosario BD, Nardecchia S, Colli MD, Devirgiliis LC, Dentini M (2008) Biomacromolecules 9:2844
22. Mitra D, Bhattacharya SC, Moulik SP (2008) J Phys Chem B 112:6609

23. Akbulut M, Reddy NK, Bechtloff B, Koltzenburg S (2008) Langmuir 24:9636
24. Cosgrove T, Hone JHE (1998) Langmuir 14:5376
25. Lin SY, Wu TF, Tsao HK (2003) Macromolecules 36:8786
26. Miller DD, Lenhart W, Antalek BJ, Williams AJ, Hewitt JM (1994) Langmuir 10:68
27. Whitesides TH, Miller DD (1994) Langmuir 10:2899
28. Saxena A, Antony T, Bohidar HB (1998) J Phys Chem B 102:5063
29. Howe AM (2000) Curr Opin Colloid Interface Sci 5:288
30. Liu XH, Kan C, Wang X, Yang XJ, Lu LD (2006) J Am Chem Soc 128:430
31. Eysturskarð J, Haug IJ, Ulset AS, Draget KI (2009) Food Hydrocoll 23:2315
32. Liu XH, Yan TT (1995) Chem J Chin Univ 16:156
33. Lin YC, Hsu CH, Lin HP, Tang CY, Lin CY (2007) Chem Lett 36:1258
34. Sun LB, Kou JH, Chun Y, Yang J, Gu FN, Wang Y, Zhu JH, Zou ZG (2008) Inorg Chem 47:4199
35. Prouzet E, Pinnavaia TJ (1997) Angew Chem Int Ed Engl 36:516
36. Sung-Suh HM, Luan ZH, Kevan L (1997) J Phys Chem B 101:10455
37. Sing KSW, Everett DH, Haul RAW, Moscou L, Pierotti RA, Rouquerol J, Siemieniewska T (1985) IUPAC 4:603
38. Belmabkhout Y, Sayari A (2009) Adsorption 15:318
39. Mizutani M, Yamada Y, Nakamura T, Yano K (2008) Chem Mater 20:4777
40. Suzuki TM, Mizutani M, Nakamura T, Akimoto Y, Yano K (2008) Microporous Mesoporous Mater 116:284
41. Monnier A, Schueth F, Huo Q, Kumar D, Margolese D, Maxwell RS, Stucky GD, Krisnamurty M, Petroff P, Firouzi A, Janicke M, Chmelka BF (1993) Science 261:1299
42. Huo QS, Margolese DI, Ciesla U, Feng PY, Gier T, Sieger P, Leon R, Petroff PM, Schüth F, Stucky GD (1994) Nature 368:317